Electron-trapped centers in x-irradiated LiCl:Fe crystals

S. V. Nistor, I. Ursu, and M. Velter-Stefanescu
Central Institute of Physics, P.O. Box MG-6 Magurele, Bucuresti 76900, Romania
(Received 13 August 1986; revised manuscript received 25 November 1986)

Single crystals of LiCl containing 140 ppm Fe^{2+} exhibit after x irradiation at 77 K ESR signals attributed to Fe^{+} centers. Designated $Fe^{+}v_c$(NN), $Fe^{+}v_c$(NNN), and Fe^{+}, they are identified with respectively a substitutional Fe^{+} ion perturbed by a nearest- and a next-nearest-neighbor cation vacancy and an isolated Fe^{+} ion without any near defect. Simultaneous thermal decay of the first two types, present in a 5:1 ratio, occurs between 120 and 150 K as the perturbing vacancy moves away. A corresponding increase in the concentration of Fe^{+} centers with the perturbing vacancy located farther away, and finally of unperturbed Fe^{+}, is observed. An activation energy of 0.46 eV for the free movement of the cation vacancy in LiCl is estimated. The crystal-field theory of Tinkham and the point-charge approximation is successfully applied to the noncubic Fe^{+} centers in LiCl:Fe, NaCl:Fe, and NaF:Fe. The presence of other ESR lines, tentatively attributed to Fe^{+} ions perturbed by near silicon ions, incorporated in the lattice during the crystal growth, is reported. No Fe^{+} centers were observed in KCl:Fe and RbCl:Fe crystals.

I. INTRODUCTION

Electron-spin-resonance (ESR) studies have shown[1,2] that iron-group ions are usually incorporated in alkali halides substitutionally, on a cation site in a divalent charge state, the excess charge being compensated by additional cation vacancies (v_c). A large fraction of the v_c's are located either in the nearest-neighbor (NN) or in the next-nearest-neighbor (NNN) position, as earlier observed by Watkins in his classical work on Mn^{2+}-doped alkali chlorides.[3] A similar behavior would be expected for alkali halides doped with iron. Unfortunately, Fe^{2+} which seems to be the normal valency state of substitutional iron, is difficult to observe by ESR spectroscopy, even at liquid-helium temperature (LHeT), due to strong line-broadening effects.[4] As will be shown here, the difficulty in detecting Fe in LiCl by ESR is overcome by x-irradiating at liquid-nitrogen temperature (LN_2T). In such circumstances the ESR spectra of Fe^{+} centers reveal the presence, location, and diffusion of charge-compensating cation vacancies in the crystal lattice.

II. EXPERIMENTAL PROCEDURE

Samples used in this study, of $3\times3\times10$ mm^3, were cleaved from LiCl single crystals grown in a reactive atmosphere, in closed transparent fused-silica ampoules, with 0.1 mol % metallic iron added to the melt. pA-grade (Merck) compounds were used as starting materials. Before the ampoules were closed their contents were dried to 350 °C, under a vacuum of 10^{-1} mm Hg. Afterwards, in order to remove the oxygen and oxygen-containing anions still left in the crystal lattice, purification in a reactive atmosphere[5] was performed. This was done by melting under a continuous flow of argon-containing CCl_4 vapors, injected into the substance through a small-diameter fused-silica tube. As suggested by Simonetti and McClure[6] successful purification is obtained by further warming of the melt up to 850–900 °C, besides using very pure (at least 99.999%) argon gas. Afterwards the ampoules were sealed off, cooled down to room temperature (RT), and transferred to a conventional Bridgman-type crystal-growth furnace. Opening the ampoules in a dry box, we found the as-grown crystals covered with a light-brown-green layer of iron chloride, resulting from the strong segregation of the iron in the crystal-grown process. Indeed, the concentration of iron in the samples used for ESR measurements, cleaved from the middle of the single crystals, was found by colorimetrical analysis to be only 140 ppm. The quality of the {100} cleavage planes for LiCl is much poorer than for KCl or NaCl crystals, as a result of the large amount of plastic deformation accompanying the cleaving process. Consequently, the orientation of the sample on the sample rod in the microwave cavity is more difficult to accomplish.

To disperse the Fe^{2+}-v_c complexes, expected to form in the crystal as a result of the aggregation process, the samples to be studied were heated to 500 °C for 5 min and quenched by dropping onto a brass block. Besides dispersing the impurity–cation-vacancy pairs, such treatment makes the samples more suitable for trapping electrons, holes, and interstitial halogen atoms.

After quenching, the LiCl:Fe samples were covered with a shallow light-brown-russet layer rich in iron, due to its fast tendency to diffuse to the crystal surface during sample heating. The corresponding variation in the iron content increases the difficulties in doing quantitative ESR measurements as a function of the irradiation time or other optical and thermal treatments.

An x-ray tube with tungsten target and beryllium windows, operating at 50 kV and 35 mA, was used for x-irradiation. The samples were placed at 6 cm from the tube window, in a quartz Dewar with thin walls, filled with liquid nitrogen.

The ESR measurements were performed at 4.2 K, with a homodyne spectrometer equipped with reference arm,

operating in the 9-GHz microwave band, at 100-KHz magnetic field modulation.[7] The microwave cavity, of immersion type, cylindrical (TE_{011} mode), allows measurements to be performed in the (1.4–300)-K temperature range and the samples to be replaced even when the Dewars contained cryogenic liquid. The temperature of the sample is continuously monitored with Au–0.03 wt. % Fe versus Chromel or copper versus Constantan thermocouples inserted in the sample supporting rod. *In situ* pulse-annealing experiments can be performed just by lifting the supporting rod with the sample at various heights above the liquid-He level. The main difficulty in performing such experiments is the presence of a temperature gradient between the sample and the thermocouple, located approximately 1.5 cm above the specimen. However, by adequate calibration the error does not exceed 5 K.

As the activation temperature for the movement of vacancies and holes in LiCl is close to LN_2T, the transfer from the irradiation Dewar into the microwave cavity should be performed in such a way as to avoid any warm-up of the sample. This has been achieved by firstly inserting the sample in the holder, made from Teflon, with one end closed and screwing the other end to the supporting rod, all operations being made under liquid nitrogen. During the subsequent transfer in the microwave cavity, which takes only a few seconds, the small amount of liquid nitrogen left in the sample holder is enough to keep the temperature of the sample around 77 K.

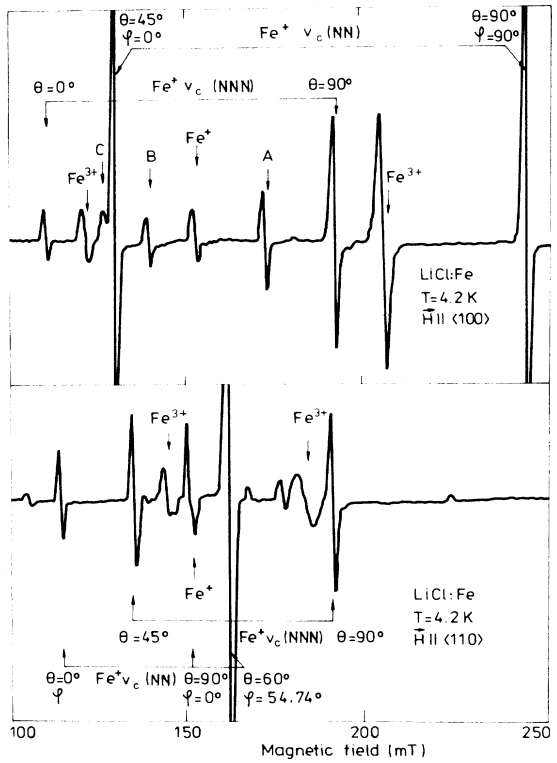

FIG. 1. The ESR spectrum of LiCl:Fe crystals x-irradiated 2 h at LN_2T, recorded in the x-band at 4.2 K, for $\mathbf{H}\|\langle 100\rangle$ and $\langle 110\rangle$.

III. RESULTS

A. The ESR spectra

No ESR transitions have been observed before x-irradiating the samples, which suggests that the iron enters the LiCl lattice as Fe^{2+}. After relatively short exposures to x-rays at LN_2T, a strong, anisotropic spectrum is observed. Figure 1 presents the ESR spectra of LiCl:Fe crystals for $\mathbf{H}\|\langle 100\rangle$ and $\langle 110\rangle$, after 1 h of x-irradiation at LN_2T. Such spectra were usually recorded at microwave power levels of less than 10^{-5} W to avoid saturation effects. It should be noted that in the case of similar centers in NaCl (Refs. 8 and 9) saturation occurs even at microwave power levels as low as 4×10^{-7} W.

From the angular dependence of the ESR transitions (Fig. 2) three main electron-trapped Fe^+-type centers with respectively orthorhombic symmetry along $\hat{\mathbf{x}}\|\langle 1\bar{1}0\rangle$, $\hat{\mathbf{y}}\|\langle 001\rangle$, and $\hat{\mathbf{z}}\|\langle 110\rangle$, tetragonal (axial) symmetry around $\hat{\mathbf{z}}\|\langle 001\rangle$ and cubic (isotropic) symmetry, were found. The identification of their structure is quite straightforward if one takes into consideration the symmetry properties of the corresponding ESR spectra, as well as by comparison with previous results concerning Fe^+ centers in alkali halides.[9–12] The orthorhombic center consists of a substitutional Fe^+ ion with a v_c located in the NN position and it will be further designated Fe^+v_c(NN). The tetragonal Fe^+ center differs only in that the v_c is located in a NNN position and it will be further designated Fe^+v_c(NNN). The cubic Fe^+ consists simply of a substitutional Fe^+ ion with no perturbing defect in the neighborhood. There are six and three equally probable orientations of the Fe^+v_c(NN) and Fe^+v_c(NNN) centers, respectively, in the lattice. As will be shown, the proposed structural models are supported by the analysis of the ESR spectra and by the pulse-annealing experiments.

No hyperfine splitting from the nuclei of the ^{57}Fe isotope ($I=\frac{1}{2}$, natural abundance 2.3%) has been observed, even in samples doped with iron containing 95% of the ^{57}Fe isotope. It means that the hyperfine splitting is smaller than the ESR linewidth ($\Delta H=1.3\pm0.2$ mT).

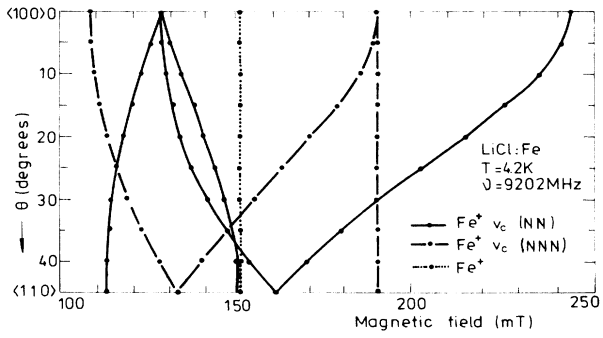

FIG. 2. Angular variation in a $\{100\}$ plane of the ESR transitions of Fe^+ centers in LiCl crystals, for a microwave frequency of 9.2 GHz. Both experimental points and calculated variation are presented.

The ESR spectra for all Fe^+ centers were fitted to the spin Hamiltonian:

$$\mathcal{H}_s = \beta \mathbf{H} \cdot \tilde{\mathbf{g}} \cdot \mathbf{S} \tag{1}$$

with $S = \frac{1}{2}$. The results are presented in Table I, together with data on Fe^+ centers in other alkali halides.

The theoretical interpretation follows a well-established pattern.[12,13] In an octahedral crystal field the ground term $^4F_{3/2}$ of a $d^7(Fe^+)$ configuration is split into a Γ_2 singlet and two triplets Γ_4 and Γ_5, the triplet Γ_4 being the lowest. The spin-orbit coupling lifts the $3\times 4 = 12$-fold degeneracy of Γ_4, leaving a Kramers doublet, to which corresponds a fictitious spin $S' = \frac{1}{2}$ as the ground state. The g value of this ground state is given by

$$g = \tfrac{5}{3} g_s - \tfrac{2}{3} \tilde{g}_l \simeq 4.33 \tag{2}$$

where $g_s = 2.0023$ is the spin contribution and $g_l = -\frac{3}{2}$ is the orbital contribution.

The effect of the axial (tetragonal and trigonal) crystal fields consists[13] in mixing of excited levels into the ground one, the g components being connected by the formula

$$g_\parallel + 2g_\perp = 5g_s - 2\tilde{g}_l = 3g \simeq 13 \ . \tag{3}$$

As can be easily checked, the g values presented in Table I are in fairly good agreement with (2) and (3). The observed deviations may be attributed[13] to the mixing by the cubic crystal field of the excited ^4P term in the ^4F ground term. However, covalency effects should be considered, too, and this could be formally taken care of[12] by substituting $\tilde{g}_l$ with $k\tilde{g}_l$, where k is a covalency (or charge-transfer) reduction factor.

Besides the possible charge transfer, a complete analysis of the Fe^+-center ESR spectra should take into consideration the presence of rhombic crystal fields. Tinkham[14] has solved this problem in an approximate manner, by considering first the effect of the spin-orbit coupling and treating the noncubic crystal field as a perturbation. For an electron with coordinates x_1, x_2, x_3 relative to the impurity nucleus, situated in the orthorhombic crystalline potential

$$V_{cr} = A_2^0(3x_1^2 - r^2) + A_2^2(x_2^2 - x_3^2) \tag{4}$$

the g components are given by

$$\begin{aligned} g_1 &= (\tfrac{10}{3} + k) - 2a(\tfrac{4}{3} + k) \ , \\ g_2 &= (\tfrac{10}{3} + k) + (a + r)(\tfrac{4}{3} + k) \ , \\ g_3 &= (\tfrac{10}{3} + k) + (a - r)(\tfrac{4}{3} + k) \ . \end{aligned} \tag{5}$$

Here the x_1 axis is parallel to a $\langle 001 \rangle$ crystalline direction, which corresponds to the y axis in our former notation.[9] In an analogous way x_2 corresponds to the z axis and x_3 to the x axis. In Eqs. (5) a and r represent the effect of axial and rhombic distortions, expressed in units of the spin-orbit coupling constant λ:

$$a = -\frac{16 A_2^0 \langle r^2 \rangle \, |e|}{315\lambda} \ , \tag{6a}$$

$$r = \frac{4 A_2^2 \langle r^2 \rangle \, |e|}{315\lambda} \ . \tag{6b}$$

The values of a, r, and k, determined according to Eqs. (5), are given in Table II. As will be further discussed, these parameters can be explained with the ionic point-charge model of the crystal field.

Besides the ESR lines attributed to the above mentioned Fe^+ centers, additional lines were observed after x-irradiation at LN_2T. By analogy with the studies on x-irradiated NaCl:Fe crystals,[8,15] the ESR lines exhibiting extremely strong anisotropy and larger linewidths (~ 2 mT) are attributed to hole-trapped Fe^{3+} centers.

Several ESR lines, exhibiting similar linewidths as those attributed to the Fe^+ centers, but lower intensities, can be also seen around $g = 4.3$. The angular dependence of these lines cannot be clearly followed due to overlap with the stronger lines of the Fe^+ centers. However, as shown in Fig. 1, for $\mathbf{H} \| \langle 100 \rangle$ a strong degeneracy is observed with only the three lines denoted by A, B, and C being left.

B. Pulse-annealing experiments

From the intensities of the ESR lines one finds the concentration of $Fe^+ v_c$(NN) to be about 5 times larger than

TABLE I. Spin Hamiltonian parameters of the Fe^+ centers in LiCl and NaCl [For the $Fe^+ v_c$(NN) center in NaCl a value of $g_l = 2.600$ should be considered at 20 K. By error a different value was printed in Ref. 9.] determined at 4.2 K, as well as the earlier reported[11,12] data in NaF and LiF obtained at 20 K.

Center	Host	$g_l(\langle 001 \rangle)$	$g_2(\langle 110 \rangle)$	$g_3(\langle 1\bar{1}0 \rangle)$
Fe^+(NN)	NaF	2.029±0.002	5.792±0.002	4.585±0.002
(orthorhombic)	LiCl	2.722±0.001	5.702±0.005	4.365±0.002
	NaCl	2.603±0.001	6.130±0.006	4.213±0.003
$Fe^+ v_c$(NNN)	LiCl	$g_\parallel = 5.924 \pm 0.005$	$g_\perp = 3.467 \pm 0.003$	
(tetragonal)	NaCl	$g_\parallel = 6.756 \pm 0.006$	$g_\perp = 3.105 \pm 0.003$	
Fe^+	LiF		$g = 4.251 \pm 0.002$	
(cubic)	NaF		$g = 4.351 \pm 0.001$	
	LiCl		$g = 4.339 \pm 0.003$	
	NaCl		$g = 4.400 \pm 0.003$	

TABLE II. Crystal-field parameters of the noncubic Fe^+ centers in some alkali halides determined with the g values given in Table I.

Center	Host	R (Å)	a	r	k	a_0	$\xi(a/r)$	$\eta(a)$	ξ^+	ξ_p
Fe^+v_c(NN)	NaF	2.304	0.493	0.283	0.802	0.180	0.156		0.111	0.070
	LiCl	2.546	0.340	0.295	0.930	0.132	0.191		0.072	0.179
	NaCl	2.798	0.370	0.414	0.982	0.100	0.220		0.076	0.135
Fe^+v_c(NNN)	LiCl	2.546	−0.358		0.930			0.118	0.111	0.179
	NaCl	2.798	−0.525		0.982			0.270	0.076	0.135

that of Fe^+v_c(NNN), while the cubic Fe^+ represents only a few percent of the total amount of Fe^+ centers. The relative concentration of the Fe^+ centers can be strongly changed by subsequent warmup, as shown by the pulse-annealing experiments (Fig. 3). In the 77–120 K temperature range all paramagnetic centers are stable. Upon warming the crystal above 120 K, one observes a drop in the intensity of both Fe^+v_c(NN) and Fe^+v_c(NNN) centers and an increase in the intensity of cubic Fe^+. We assume the intensity variations, associated with changes in the concentration of various centers involved, are determined by the thermally activated movement of the perturbing v_c away from the Fe^+ ion, movement which is not anymore hindered by the Coulombian attraction of the precursor Fe^{2+} extrapositive charge. With notations employed by Delbecq *et al.*[16] to describe such processes in KCl:Sn^+, the decay of the Fe^+v_c(NN) centers is attributed to the jump of perturbing v_c from the (1,1,0) position to the (2,0,0) position and the decay of Fe^+v_c(NNN) to the v_c jumping from (2,0,0) to (2,1,1) or (3,1,0). In the case of the LiCl, both movements involve similar activation energies.

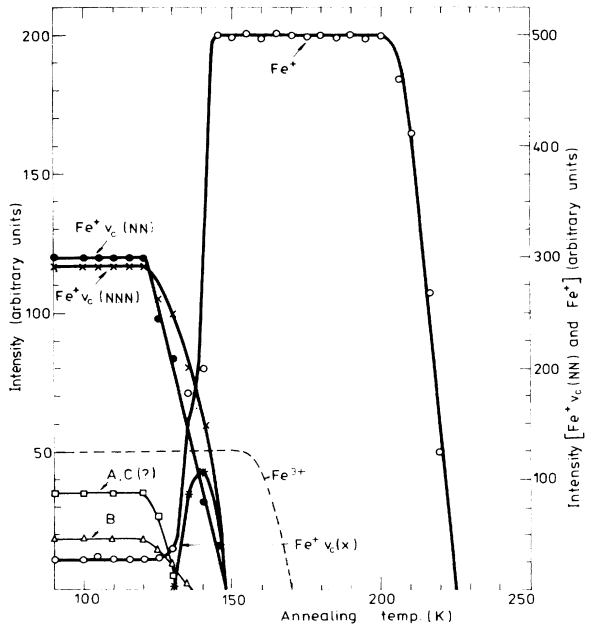

FIG. 3. Pulse-annealing data of a LiCl:Fe sample which had been x-irradiated at LN_2T for 2 h. The sample was warmed to the temperature indicated by the data point, held there for 5 min and the spectrum ($\mathbf{H}\|\langle 100\rangle$) recorded at 4.2 K. The relative intensities of various centers presented are arbitrary.

It is expected that the Fe^+v_c centers with the v_c located farther away than the NNN position, but still causing sensible perturbation at the Fe^+ site, would represent paramagnetic centers with lower symmetry and consequently more complicated ESR spectra. According to our knowledge such centers have not been observed yet by ESR spectroscopy.

In the LiCl:Fe crystals a new group of ESR lines is produced by pulse-annealing above 125 K. This group of anisotropic lines is centered on the ESR line attributed to cubic Fe^+ centers (Fig. 4). Owing to overlap between various components no angular dependence could be obtained. Based on pulse-annealing data, tentatively we assign these ESR lines to centers designated $Fe^+v_c(x)$ with the perturbing v_c situated farther away than the NNN sites. This identification is supported by the following arguments:

(a) The corresponding centers exhibit ESR spectra centered around $g=4.3$ with smaller g anisotropies compared to Fe^+v_c(NN) and Fe^+v_c(NNN). Such features would result from smaller noncubic crystal fields acting on the Fe^+ ion, as expected from a perturbing v_c situated farther away from the Fe^+ ion.

(b) The concentration of $Fe^+v_c(x)$ exhibits a sharp increase above 130 K, reaching the maximum at 140 K. In the same temperature range the concentration of cubic Fe^+ changes slowly. Above 140 K the concentration of cubic Fe^+ exhibits a dramatic increase, which is accompanied by the sharp decay and disappearance of the whole

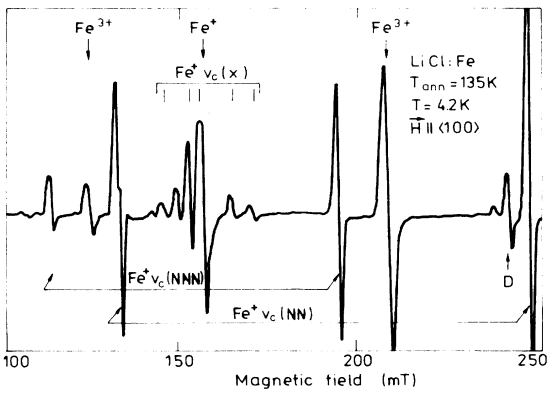

FIG. 4. The ESR spectrum of a LiCl:Fe sample x-irradiated 2 h at LN_2T and subsequently pulse annealed up to 135 K for $\mathbf{H}\|\langle 100\rangle$. The A (C) and B centers have decayed completely. ESR transitions attributed to $Fe^+v_c(x)$ centers, consisting of Fe^+ ions with perturbing cation vacancy situation at lattice points farther away than the NNN position, can be observed in the central part.

group of ESR lines attributed to $Fe^+v_c(x)$ centers. The variation in the concentration of cubic Fe^+, on the background provided by the continuous decay of the Fe^+v_c(NN) and Fe^+v_c(NNN) centers, can be understood if one accepts the presence of an intermediate step, consisting of such stable $Fe^+v_c(x)$ centers.

The relative concentration of the centers responsible for the *A*, *B*, and *C* lines is substantially altered by a subsequent warmup, as shown in Fig. 3. Above 120 K their intensity decreases. However, *A* and *C* exhibit a faster decay compared to *B*, the former (*A* and *C*) vanishing around 132 K and the latter (*B*) around 137 K. It should be mentioned that the intensity of the *C* line is quite difficult to monitor accurately being partly hidden under the much stronger $\vartheta=45°$, $\varphi=0°$ transition of the Fe^+v_c(NN) centers. The pulse-annealing experiments show clearly that at least two paramagnetic centers are responsible for (*A* and *C*) and *B* lines, respectively. The concentration of both $Fe^+v_c(x)$ and Fe^+ centers still increases after the complete decay of *A* (*C*) and *B*. It means that the paramagnetic centers responsible for these lines do not represent precursors of $Fe^+v_c(x)$ and cubic Fe^+ centers.

IV. DISCUSSION

From the analysis of both ESR spectra and pulse-annealing experiments, we believe the evidence is rather convincing that by x-irradiation at LN_2T three main Fe^+ centers, i.e., Fe^+v_c(NN), Fe^+v_c(NNN), and isolated cubic Fe^+ are formed. They result from trapping of electrons produced by x-irradiation at substitutional Fe^{2+} ions, most of which are associated with charge compensating v_c situated in NN and NNN positions. Assuming that the trapping of an electron by Fe^{2+} will not change the relative position of the vacancy and the iron, and the spin-lattice relaxation of all Fe^+ centers is quite similar, one may conclude that in our samples the concentration of the $Fe^{2+}v_c$(NN) impurity complex is about 5 times larger compared to the $Fe^{2+}v_c$(NNN), and then together they make up more than 95% of the Fe^{2+} dissolved in the lattice. Comparing with the corresponding value of 1.3 found in NaCl:Fe crystals,[10] one concludes that in LiCl:Fe, the NN position of the charge compensating v_c is energetically much more favored. To what extent this ratio may be influenced by the thermal treatment of the sample before irradiation and the total concentration of iron remains to be studied, since the formation of dimers, trimers, etc., of Fe^{2+}-v_c complexes cannot be neglected. Moreover, it should be mentioned that a sizable amount of Fe^{2+} ions present in the crystal lattice act as hole-trapping centers, a fact which has been already observed in NaCl:Fe crystals.[8,15] It is not yet clear whether the Fe^{3+} centers originate from isolated Fe^{2+}-v_c complexes too, from higher aggregation states of such complexes, or from Fe^{2+} ions located in other specific sites of the lattice (like interstitial positions).

A. Vacancy migration near Fe^+

It has been found that by warming the crystals previously x-irradiated at LN_2T, the perturbing v_c, which is not anymore bound by Coulombian forces to the iron ion, moves away, as reflected in the ESR spectra. If one assumes that migration of the v_c through the lattice occurs as a series of elementary jumps from one cation site to the nearest-neighbor site,[16] the conversion of noncubic Fe^+ to cubic Fe^+ results from successive jumping away of the v_c from a NN to a NNN position near Fe^+ and then further away.

When the x-irradiated crystal is warmed, no visible changes in the intensity of various ESR transitions are visible up to 120 K. Above this temperature both Fe^+v_c(NN) and Fe^+v_c(NNN) centers decay, as the v_c jumps away, finally resulting in isolated Fe^+ ions at sites with cubic symmetry. However, in the narrow temperature range below 140 K, a sizable amount of Fe^+ centers, called $Fe^+v_c(x)$, which seem to be due to the presence of the perturbing v_c situated farther away from the Fe^+, are formed. Limiting ourselves to the next three sites, the location of the perturbing v_c in various such positions would yield centers with C_s symmetry, if the v_c is situated in the (2,1,1) or (3,1,0) sites, respectively, C_{2v} for the v_c situated in the (2,2,0) positions. As the energy barrier for moving farther away from such positions must be very small, a large amount of isolated Fe^+ is already produced for $T<140$ K. The $Fe^+v_c(x)$ centers decay in a very narrow temperature range (a few K) above 140 K, corresponding to the complete disappearance of both Fe^+v_c(NN) and Fe^+v_c(NNN), too. The decay of all these centers is accompanied by a sharp increase in the concentration of isolated Fe^+ ions. This last process occurs in the 140–150 K temperature range. In view of the presence of intermediate $Fe^+v_c(x)$ centers, we estimate that the v_c must be displaced at least two lattice constants from the Fe^+ ion in order to give no measurable perturbing influence. Supposing that the jump of the $v_c(x)$ in the next position, farther away from the Fe^+ ion, is the rate controlling step for escape of the cation vacancy, one may estimate the corresponding energy barrier ε_e, in a similar way to Ref. 16. Neglecting in the rate equation the terms which correspond to jumps in positions nearer to the Fe^+ ion, we obtain by integration

$$\ln[N(x)N_0^{-1}(x)]=-4\nu_e t\ , \tag{7}$$

where $N_0(x)$ and $N(x)$ represent the initial and final concentration of $Fe^+v_c(x)$ centers after t seconds of warmup to the temperature T, respectively. ν_e is the escape jump frequency corresponding to the jump of $v_c(x)$ in a position farther away from the perturbing Fe^+ ion. Expressed in the Arrhenius form,

$$\nu_e=S\exp(-\varepsilon_e/kT)\ , \tag{8}$$

where S is the frequency factor.

Considering that after 5 min of pulse annealing at $T=142$ K the concentration of $Fe^+v_c(x)$ centers decreases to half, with a similar increase in the concentration of cubic Fe^+ centers and assuming $S\sim10^{13}$ sec^{-1}, the value of $\varepsilon_e=0.46\pm0.04$ eV is obtained. The corresponding error was estimated by taking into account the accuracy of our experimental data, as well as the approximations involved in the calculation.

ε_e represents the activation energy for the cation vacancy jumping in sites which are little influenced by the Fe^+ ions. Therefore it can be taken in a good approximation to be equal to the activation energy for migration of the isolated cation vacancy. Indeed, it compares reasonably well with the activation energy for migration of cation vacancies $\varepsilon_c = 0.41$ eV obtained in earlier electrical conductivity measurements.[17] The small deviation of ε_e from ε_c, might be attributed to the relaxation of the lattice ions in the neighborhood of the Fe^+ ion.

B. Description of the Fe^+ centers

The crystal-field parameters (Table II) determined according to Tinkham's theory can be further employed in discussing the models of noncubic Fe^+ centers. Such analysis, in the frame of a point-charge approximation, has been earlier performed for S-state paramagnetic ions, like Mn^{2+} (Refs. 3 and 18) and Eu^{2+} (Refs. 19 and 20) in alkali halides. The calculations have given the correct sign for both axial and orthorhombic terms, as well as the right ratio, but their absolute magnitude was almost a factor of 10 too low. Such quantitative discrepancy has been explained as being mainly due to neglecting the spatial extension of the electron clouds, including the overlap (covalency). As recently shown for Eu^{2+} in alkali halides[21] we believe a large part of this discrepancy to be due to the less accurate theoretical interpretation of the fine-structure parameters for the S-state ions. Indeed, this interpretation is not as straightforward as for the non-S-state paramagnetic ions, since it involves higher-order perturbation terms in which spin-orbit and crystal-field interactions as well as excited states are taken into consideration.[1,12] As will be shown here, for the $(3d^7)Fe^+$ ion the point-charge approximation yields values of the spin Hamiltonian parameters which are in much better agreement with the experimental values.

In a point-charge approximation the noncubic crystal field acting on the paramagnetic impurity arises both from the effective charge of the v_c and from the ionic and electronic (polarization) displacements of the neighboring ions surrounding the vacancy. Because the polarization falls off as r^{-3} from the vacancy and because the contribution from a displaced charge also falls off as r^{-3}, only the halide anions adjacent to both vacancy and Fe^{3+} are accounted for.[3]

In the orthorhombic Fe^+ center (Fig. 5) the cation vacancy is considered as a single negative charge $-e$, situated at $\sqrt{2}R$ away from the iron nucleus and the NN halide anions as single negative charges $-|e|$, displaced by ξR along the corresponding $\langle 100 \rangle$ axes, away from the position in the perfect lattice. R is the cation-anion distance at low-temperature. The parameters of the crystal-field potential (4) are thus expressed as

$$A_2^0 = \frac{|e|}{8\sqrt{2}R^3} , \tag{9a}$$

$$A_2^2 = \frac{3|e|}{R^3}\left(\frac{1}{8\sqrt{2}} - \xi\right) . \tag{9b}$$

Using these parameters in Eqs. (6) we show that for the orthorhombic Fe^+ center $a > 0$ and $r \leqq 0$ if $\xi \leqq 1/(8\sqrt{2})$, or $r > 0$ if $\xi > 1/(8\sqrt{2})$. The experimental values (Table II) exhibit the correct sign for all studied alkali halides. The calculated values of the parameter a (denoted a_0), which according to Eqs. (6a) and (9a) does not depend on the displacements of the neighboring anions, compare better with the experimental values than in the case of the S state ions, being only about three times smaller. (In all calculations we have employed, according to Ref. 12, the following parameters for the Fe^+ ion: $\lambda = -119$ cm^{-1} and $\langle r^2 \rangle = 1.774$ a.u. $= 0.5 \times 10^{-20}$ m^2). It is hard to explain such difference by overlap and charge transfer between the Fe^+ ion and its neighbors, at least for LiCl and NaCl, where covalency is negligible (the orbital reduction factor $k \sim 1$). The difference could be explained rather as a result of neglecting in the point-charge approximation the nonspherical spatial extension of the electron clouds surrounding the Fe^+ and v_c. Accepting such effect to be manifested similarly for both axial and orthorhombic components of the crystal field, one should obtain from the ratio a/r a better fitting between theory and experiment. Indeed, the numerical values of the ionic displacement ξ compare fairly well with the theoretical calculations[22] of the ionic displacements ξ^+ around a cation vacancy (Table II). One should remember that ξ represents the combined ionic and electronic displacements. The last one can be evaluated in a rather crude way in the point-charge approximation by considering the electronic polarization ξ_p as induced at the neighboring anions by the $-|e|$ charge concentrated at the center of the cation vacancy. By simple manipulations one finds $\xi_p = \alpha/R^3$, where α is the electronic polarizability. The values obtained by adding ξ^+ to ξ_p (Table II) are in a good agreement with ξ, considering all the approximations involved.

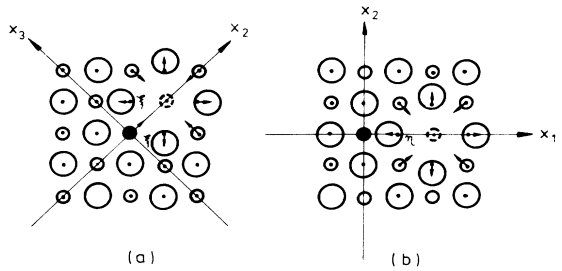

FIG. 5. Models of the (a) Fe^+v_c(NN) and (b) Fe^+v_c(NNN) centers in alkali halides, in a {100} plane. The solid circle is Fe^+, the large and small circles are, respectively, anions and cations, and the dashed circle is the cation vacancy. The nearest anions surrounding the vacancy are shown in the displaced positions. For the nearest cations only the directions of the displacements are shown.

In the case of the axial Fe^+ center the v_c is in a $\langle 100 \rangle$ direction [Fig. 5(b)], farther away from the Fe^+ ion. Considering only the displacement ηR of the anion adjacent to both v_c and Fe^+, plus the effect of the v_c as a single negative charge $-|e|$ situated at $2R$ from the Fe^+ ion, the point-charge approximation gives

$$A_2^0 = -\frac{|e|}{16R^3}(3 + 72\eta) , \tag{10a}$$

$$A_2^2 = 0 \ . \tag{10b}$$

Consequently, $a < 0$, as is the case (Table II) for both LiCl and NaCl, for which experimental data are available. Owing to the larger distance between the paramagnetic ion and the charge compensating vacancy, it is expected that the errors from neglecting the spatial extension of the electron clouds and from treating the v_c as a point charge to be less important. Indeed, we find (Table II) from (10a) values of η which are in good agreement with the theoretical values of ξ^+ and ξ_p.

Comparing the anion displacements in the axial and orthorhombic Fe^+ centers, one finds $\xi > \eta$ for LiCl and $\xi < \eta$ for NaCl (Table II). Considering such displacement to be due to the presence of the adjacent compensating v_c, one would expect for a perfect lattice $\xi = \eta$ in both cases. The observed differences seems to be due to the presence of the nearby Fe^+ ion, which has a larger radius (0.8×10^{-10} m) compared to Li^+ (0.68×10^{-10} m) and a smaller one compared to Na^+ (0.97×10^{-10} m).[23] (After our knowledge the crystalline ionic radius of Fe^+ has not been determined. We have taken as ionic radius $R_0 = f\langle r^2 \rangle_d$. The normalization factor $f = 1.15$ is obtained from the known[23] ionic radii of Fe^{2+} and Fe^{3+}). Indeed it is expected that for LiCl the anion located between the compensating v_c and the Fe^+ ion will relax outward less in the axial center, compared to the relaxation of the two adjacent anions in the orthorhombic center, due to the opposition from the larger Fe^+ in the former case. A contrary effect would be expected for NaCl, as the smaller Fe^+ will give more room to the adjacent anion in the axial center to relax outward.

V. CONCLUSIONS

We have inferred that iron dissolves in LiCl crystals as Fe^{2+} because ESR spectra assigned to Fe^+ and Fe^{3+} centers are observed only after x-irradiation at LN_2T. The corresponding orthorhombic $Fe^+ v_c$(NN), tetragonal $Fe^+ v_c$(NNN), and cubic Fe^+ are identified with, respectively, a substitutional Fe^+ perturbed by a nearest and a next-nearest cation vacancy and an isolated substitutional Fe^+ ion. It is concluded from this study that in crystals quenched before x-irradiation, Fe^{2+} perturbed by the nearest and next-nearest cation vacancies occur in a ratio of 5:1 and taken together they make up more than 95% of the Fe^{2+} dissolved in the lattice. Thermal decay of the $Fe^+ v_c$(NN) and $Fe^+ v_c$(NNN) occurs simultaneously in the 120–140 K temperature range, as the perturbing v_c jumps further away. This decay is accompanied by the production of several ESR lines with small anisotropy centered at $g = 4.33$, attributed to $Fe^+ v_c(x)$ centers with the perturbing v_c bound farther away than the (2,0,0) position, in the neighborhood of the Fe^+ ion. Above 140 K the v_c becomes free, moving away completely, with a corresponding sharp increase in the concentration of cubic Fe^+. It has been estimated that the activation energy for the free-cation vacancy motion in the LiCl lattice is 0.46 ± 0.04 eV. This value compares fairly well with the value of 0.41 eV obtained from electrical conductivity measurements,[17] if one takes into consideration the errors involved[24] in the latter measurements.

The ESR spectra of LiCl:Fe crystals x-irradiated at LN_2T exhibit some broader, strongly anisotropic lines, attributed to hole-trapped Fe^{3+} centers, as well as weaker lines with the same linewidths as those belonging to the Fe^+ centers, identified with *A*, *B*, and *C* in the $H \| \langle 100 \rangle$ spectrum (Fig. 4). From the thermal decay curves it has been found that *A* and *C* belong to a certain paramagnetic center and *B* to a different one. Owing to overlap no identification based on angular dependence was possible. The corresponding paramagnetic centers are tentatively identified as Fe^+ ions perturbed by certain near impurities. Such assignment is supported by the following arguments: (i) The corresponding ESR spectra are centered around $g = 4.3$, in agreement with Eqs. (2) and (3). (ii) Single crystals grown with LiCl and iron from various sources exhibit identical ESR spectra. Such identification still raises the question concerning the nature of the perturbing impurity. Even with the little information available only two possibilities are to be considered: either a neighboring iron ion originating from the presence of Fe_2^+-v_c dimers or trimers, or another impurity. To check the first alternative, LiCl:Fe samples have been quenched, after heating to 500 °C, directly in liquid nitrogen, and afterwards x-irradiated at LN_2T. It is expected that such treatment would yield a different concentration of precursor Fe^{2+}-v_c pairs in various aggregation stages, reflected in a change into the intensity of the corresponding ESR lines. However, such changes have not been observed. The second alternative is even more puzzling as LiCl:Fe samples with LiCl and iron from various sources, including Suprapur grade (Merck) LiCl, exhibit identical spectra in both line positions and relative intensities. Indeed, it is expected that the concentration of the unknown impurity originating in the starting LiCl and iron to change in some samples, which would be reflected in the relative intensities of the corresponding ESR lines. The only remaining source of impurities to be considered were the crystal-growth ampoules themselves. Because they were made from high-purity fused silica (vitreosil grade), one should consider silicon itself as the unknown impurity. Such identification is supported by the presence of silicon in the LiCl:Fe samples, as revealed from spectrochemical analysis, and by the absence of any superhyperfine structure in the corresponding ESR lines.

It is worth mentioning that in contrast to LiCl:Fe and NaCl:Fe, all our attempts to observe Fe^+ centers in x-irradiated KCl:Fe and RbCl:Fe grown in similar conditions have been unsuccessful, although the iron was present in the crystal lattices in sufficiently high concentration, as observed by the spectrochemical analysis.

ACKNOWLEDGMENTS

Thanks are due to Mrs. C. Dan and E. Apostol for the colorimetrical analysis, and to Mrs. C. D. Mateescu for help in preparing the samples and for the spectrochemical analysis.

[1]I. Ursu, *La Resonance Paramagnetique Electronique* (Dunod, Paris, 1968).
[2]N. Narayana, V. S. Sivasankar, and S. Radhakrishna, Phys. Status Solidi B **105**, 11 (1981).
[3]G. D. Watkins, Phys. Rev. **113**, 79 (1959).
[4]D. H. McMahon, Phys. Rev. **134**, A128 (1964).
[5]M. Lebl and J. Trnka, Z. Phys. **186**, 128 (1965).
[6]J. Simonetti and D. S. McClure, J. Chem. Phys. **71**, 793 (1979).
[7]M. Velter-Stefanescu and S. V. Nistor, J. Phys. E (to be published).
[8]S. V. Nistor, I. Ursu, and M. Velter-Stefanescu, in *Proceedings of the XXII Congress AMPERE, Zurich, 1984,* edited by K. A. Müller, R. Kind, and J. Ross (Zurich University Press, Zurich, 1984), p. 206.
[9]S. V. Nistor, M. Velter-Stefanescu, and C. D. Mateescu, Solid State Commun. **53**, 989 (1985).
[10]B. R. Yang, A. Bowen, and D. Schoemaker, Phys. Status Solidi B **127**, 657 (1985).
[11]T. P. P. Hall, W. Hayes, R. W. H. Stevenson, and J. Wilkens, J. Chem. Phys. **39**, 35 (1963).
[12]A. Abragam and B. Bleaney, *Electron Paramagnetic Resonance of Transition Ions* (Clarendon, Oxford, 1970).
[13]A. Abragam and M. H. L. Pryce, Proc. R. Soc. London Ser. A **206**, 173 (1951).
[14]M. Tinkahm, Proc. R. Soc. London, Ser. A **236**, 549 (1956).
[15]S. V. Nistor, I. Ursu, and M. Velter-Stefanescu, Phys. Status Solidi B **135**, K149 (1986).
[16]C. J. Delbecq, R. Hartford, D. Schoemaker, and P. H. Yuster, Phys. Rev. B **13**, 3631 (1976).
[17]Y. Haven, Rec. Trav. Chim. **69**, 1471 (1950).
[18]Y. Yokozawa and Y. Kazumata, J. Phys. Soc. Jpn. **16**, 694 (1961).
[19]M. Sumita, K. Kawano, and R. Nakata, J. Phys. Chem. Solids **39**, 557 (1978).
[20]T. Iwasaki, Y. Nakamura, and H. Wakabayashi, J. Phys. Soc. Jpn. **50**, 563 (1981).
[21]B. D. Shanina and E. N. Kalabuchova, Phys. Scr. **19**, 347 (1979).
[22]J. R. Hardy and A. M. Karo, *The Lattice Dynamics and Statics of Alkali Halides* (Plenum, New York, 1979).
[23]*Handbook of Chemistry and Physics,* 53rd ed. (The Chemical Rubber Co., Cleveland, 1973).
[24]L. W. Barr and A. B. Lidiard, in *Physical Chemistry-An Advanced Treatise,* edited by H. Eyring, D. Henderson, and W. Jost (Academic, New York, 1970), Vol. 10.